Backscattering of electromagnetic and gravitational waves off Schwarzschild geometry

Janusz Karkowski, Edward Malec
Institute of Physics, Jagiellonian University, 30-059 Kraków, Reymonta 4, Poland

and Zdobysław Świerczyński
Institute of Physics, Pedagogical University, 30- Kraków, Podchorążych 1, Poland

This paper shows that the backscattering of electromagnetic and gravitational waves can be dominant when the radiation is produced very close to a spherical black hole. Numerical investigation shows that almost 50 percent of the outgoing quadrupole gravitational wave is backscattered, for a class of initial data. A similar analysis reveals at least 20 percent effect for a dipole electromagnetic radiation. Numerical results confirm theoretical predictions that the backscatter of short wavelength radiation is negligible. In the long-radiation band is observed a rather weak dependence on the wavelength. Our studies base on the linear approximation. They can be of relevance for the determination of the total energy of backscattering tails and quasinormal modes.

04.20.-q 04.30.Nk 04.40.-b 95.30.Sf

I. INTRODUCTION

This paper is dedicated mainly to a numerical investigation of the backscattering ([1] - [11]) of waves in a Schwarzschild spacetime. It supplements the earlier analytic studies of scalar [12], electromagnetic ([13], [14]) and gravitational fields [16]). We study the propagation of the electromagnetic and (even-parity) gravitational waves in a background Schwarzschild spacetime. It is assumed that initial data describe an isolated pulse (burst) of a (gravitational or electromagnetic) wave. As in the earlier studies ([12], [13] and [16]) the strength of the backscattering is assessed by finding the fraction of the initial burst energy that will not reach a distant observer in the main pulse. The numerical investigation, that is reported below, gives a quantitative evaluation of the effect.

Sec. II brings an analytic estimate of the backscattering of the electromagnetic fields. The obtained result is a substantial improvement of a former bound [14]. Sec. III is dedicated to the presentation of numerical results on the backscattering of electromagnetic fields. The effect depends both on the relative width of the initial data and on the distance. Sec. IV describes the propagation of quadrupole gravitational waves in a Schwarzschild geometry. Relevant energy formulae are defined and analytic estimates are reminded. Section V goes on with numerical studies of the backscatter of gravitational fields. Similarly as before, the backscattering happens to depend on the relative width of the initial data and on the distance. In Sec. VI we briefly review the obtained results.

The space-time geometry is defined by a Schwarzschildean line element,

$$ds^2 = -(1-\frac{2m}{R})dt^2 + \frac{1}{1-\frac{2m}{R}}dR^2 + R^2 d\Omega^2 \ , \qquad (1)$$

where t is a time coordinate, R is a radial coordinate that coincides with the areal radius and $d\Omega^2 = d\theta^2 + \sin^2\theta d\phi^2$ is the line element on the unit sphere, $0 \le \phi < 2\pi$ and $0 \le \theta \le \pi$. Throughout this paper G, the Newtonian gravitational constant, and c, the velocity of light are put equal to 1. We define the Regge-Wheeler coordinate

$$r^* = R + 2m\ln(\frac{R}{2m} - 1) \qquad (2)$$

and $\eta_r \equiv 1 - 2m/r$.

II. BACKSCATTER OF ELECTROMAGNETIC WAVES: NEW ANALYTIC ESTIMATES

We seek, following [13], a solution $\Psi(r^*, t)$ in the form

$$\Psi = \tilde{\Psi} + \delta, \qquad (3)$$

where δ satisfies the dipole equation

$$(-\partial_0^2 + \partial_{r^*}^2)\delta = \eta_R\left[\frac{2}{R^2}\delta + \frac{6mf}{R^4}\right]. \qquad (4)$$

Here

$$\tilde{\Psi}(r^*, t) = \partial_t f(r^* - t) + \frac{f(r^* - t)}{R} \qquad (5)$$

and f is an arbitrary function with support in (a, ∞). f can be uniquely determined from initial data corresponding to an initially outgoing radiation. $\tilde{\Psi}$ solves Maxwell equations in Minkowski spacetime and it corresponds to the dipole radiation. Initially $\delta = \partial_0\delta = 0$.

The energy $E_R(t)$ of the electromagnetic field Ψ contained in the exterior of a sphere of the radius R reads

$$E_R(t) = 2\pi\int_R^\infty dr\left(\frac{(\partial_0\Psi)^2}{\eta_r} + \eta_r(\partial_r\Psi)^2 + \frac{2(\Psi)^2}{r^2}\right). \qquad (6)$$

$E_a \equiv E_a(0)$ is the energy of the initial pulse. Let an outgoing null geodesic $\tilde{\Gamma}_r$ originate from a point $(r, 0)$ of

the initial hypersurface. In the Minkowski spacetime the outgoing radiation contained outside $\tilde{\Gamma}_a$ does not leak inward and its energy remains constant. In a curved spacetime some energy will be lost from the main stream due to the diffusion of the radiation through $\tilde{\Gamma}_a$.

The energy loss is equal to a line integral along $\tilde{\Gamma}_a$ (where $f = \tilde{\Psi} = 0$),

$$\delta E_a \equiv E_a - E_\infty = 2\pi \int_a^\infty dr \left[\eta_r \Big(\frac{1}{\eta_r} (\partial_0 + \partial_{r^*}) \delta \Big)^2 + \frac{2\delta^2}{r^2} \right]. \quad (7)$$

An energy $H(R,t)$ of field δ,

$$H(R,t) = \int_R^\infty dr \Big(\frac{(\partial_0 \delta)^2}{\eta_r} + \eta_r (\partial_r \delta)^2 + (\delta)^2 \frac{2}{r^2} \Big), \quad (8)$$

satisfies the "conservation" equation [13]

$$(\partial_t + \partial_r^*) H(R,t) =$$
$$-\eta_R \left[\eta_R \Big(\frac{\partial_0 \delta}{\eta_R} + \partial_R \delta \Big)^2 + \frac{2}{R^2} \delta^2 \right] - 12m \int_R^\infty dr \partial_0 \delta \frac{f}{r^4} \quad (9)$$

The integration of (9) along $\tilde{\Gamma}_a$ yields

$$H(\infty,\infty) - H(a,0) = -\frac{\delta E_a}{2\pi} - 12m \int_0^\infty dt \int_{a_t}^\infty dr \partial_0 \delta \frac{f}{r^4}; \quad (10)$$

here $(a_t, t) \in \tilde{\Gamma}_a$ and $H(\infty,\infty)$ is the asymptotic energy of the field δ. Eq. (10) implies (taking into account that $H(a,0) = 0$, due to the vanishing of initial data of the field δ) that

$$\delta E_a \leq -2\pi H(\infty,\infty) + 24\pi m \Big| \int_0^\infty dt \int_{a_t}^\infty dr \partial_0 \delta \frac{f}{r^4} \Big| \leq$$
$$24\pi m \Big| \int_0^\infty dt \int_{a_t}^\infty dr \partial_0 \delta \frac{f}{r^4} \Big|. \quad (11)$$

This integral is bounded from above by

$$24\pi m \int_0^\infty dt \sqrt{H(t)} \left(\int_{a_t}^\infty dr \frac{f^2 \eta_r}{r^8} \right)^{1/2}. \quad (12)$$

On the other hand, Eq. (9) implies

$$\sqrt{H(t)} \leq 6m \int_0^t dt \left(\int_{a_t}^\infty dr \frac{f^2 \eta_r}{r^8} \right)^{1/2}; \quad (13)$$

thus

$$24\pi m \int_0^\infty dt \sqrt{H(t)} \left(\int_{a_t}^\infty dr \frac{f^2 \eta_r}{r^8} \right)^{1/2} \leq$$
$$144\pi m^2 \int_0^\infty dt \int_0^t ds \left(\int_{a_s}^\infty dr \frac{f^2 \eta_r}{r^8} \right)^{1/2}$$
$$\left(\int_{a_t}^\infty dr \frac{f^2 \eta_r}{r^8} \right)^{1/2}. \quad (14)$$

The integrand of the external integral with respect "t" is equal to the directional derivative $\frac{d}{dt} \left[\int_0^t ds \Big(\int_{a_s}^\infty dr \frac{f^2 \eta_r}{r^8} \Big)^{1/2} \right]^2$ and the last line of the preceding equation is equal to

$$72\pi m^2 \int_0^\infty dt \frac{d}{dt} \left[\int_0^t ds \left(\int_{a_s}^\infty dr \frac{f^2 \eta_r}{r^8} \right)^{1/2} \right]^2 =$$
$$72\pi m^2 \left[\int_0^\infty dt \left(\int_{a_t}^\infty dr \frac{f^2 \eta_r}{r^8} \right)^{1/2} \right]^2 \quad (15)$$

Therefore, (11-15) imply

$$\delta E_a \leq 36 m^2 \left[\int_0^\infty dt \Big(\int_{a_t}^\infty dr \frac{2\pi f^2 \eta_r}{r^8} \Big)^{1/2} \right]^2. \quad (16)$$

One can show, using reasoning as in [14], that on the initial hypersurface $t = 0$

$$\Big| \frac{f(R, t=0)}{R - 2m} \Big| = \Big| \int_a^R \partial_r \frac{f}{r - 2m} \Big| = \Big| - \int_a^R dr \frac{r \tilde{\Psi}}{(r-2m)^2} \Big|; \quad (17)$$

this can be written, using the Schwarz inequality, as

$$\Big| \frac{f(R, t=0)}{R - 2m} \Big| \leq \left(\int_a^R dr \big(\frac{\tilde{\Psi}}{r} \big)^2 \int_a^R dr \frac{r^4}{(r-2m)^4} \right)^{1/2}. \quad (18)$$

Notice that $\int_a^R dr \big(\frac{\tilde{\Psi}}{r} \big)^2 \leq E_a/(4\pi)$. From (18) follows

$$\frac{4\pi f^2}{r^2} \leq E_a a \eta_r^2 F(\tilde{m}, y), \quad (19)$$

where

$$F(\tilde{m}, y) \equiv y - 1 + \frac{16\tilde{m}^4}{3(-y + 2\tilde{m})^3} - \frac{16\tilde{m}^4}{3(-1 + 2\tilde{m})^3} -$$
$$\frac{16\tilde{m}^3}{(-y + 2\tilde{m})^2} + \frac{16\tilde{m}^3}{(-1 + 2\tilde{m})^2} +$$
$$\frac{24\tilde{m}^2}{-y + 2\tilde{m}} - \frac{24\tilde{m}^2}{-1 + 2\tilde{m}} +$$
$$8\tilde{m} \ln \frac{y - 2\tilde{m}}{1 - 2\tilde{m}}. \quad (20)$$

Here $\tilde{m} \equiv m/a$ and $y = R/a$. Inequality (20) constitutes a refined version of Eq. (13) in [14].

Let $(R,t) \in \tilde{\Gamma}_r$. The right hand side of (20) is an increasing function of r; since $R > r$ and f is constant along $\tilde{\Gamma}_r$, one obtains

$$\frac{4\pi f^2(R,t)}{R^2} \leq E_a a \eta_R^2 F(\tilde{m}, R/a), \quad (21)$$

Define $x \equiv a_t/a$. The integrand of the right hand side of (16) is bounded, taking into account (21):

$$2\pi \int_{a_t}^{\infty} \eta_r \frac{f^2}{r^8} \leq \frac{E_a a}{2} \int_{a_t}^{\infty} \frac{\eta_r^3 F(\tilde{m}, r/a)}{r^6} dr = \frac{E_a}{2a^4} G(\tilde{m}, x). \tag{22}$$

Here $G(\tilde{m}, x) = \int_x^{\infty} dx (x - 2\tilde{m})^3 F(\tilde{m}, x)/x^9$; the rather lengthy integration can be done explicitly with the use of Mapple. The result is too long to be presented here..

The insertion of (22) into (16) leaves us with

$$\delta E_a \leq \frac{18 m^2 E_a}{a^2} \left[\int_1^{\infty} \frac{dx}{1 - \frac{2\tilde{m}}{x}} \sqrt{G(\tilde{m}, x)} \right]^2. \tag{23}$$

Here we replaced the time variable t by the radial variable r; notice that along $\tilde{\Gamma}_a$ one has $dt = dr/\eta_r$. The use of the Schwarz inequality allows one to bound (23) from above by

$$\delta E_a \leq \frac{18 m^2 E_a}{a^2} \int_1^{\infty} dx G(\tilde{m}, x) x^2 \int_1^{\infty} dx \frac{1}{(x - 2m)^2}. \tag{24}$$

That implies the following estimate for the ratio of the diffused energy by the initial energy of the pulse of radiation

$$\frac{\delta E_a}{E_a} \leq 4.5 \Big(\frac{2m}{a}\Big)^2 C(\tilde{m}) \tag{25}$$

where

$$\begin{aligned} C(\tilde{m}) = \frac{-1}{10080((-1+2\tilde{m})^4 \tilde{m}^4)} \Big(& -2760\tilde{m}^5 + 828\tilde{m}^4 + \\ & 44\tilde{m}^3 + 2352\tilde{m}^6 + 2016\tilde{m}^4 \ln(1-2\tilde{m}) + \\ & 2688\tilde{m}^6 \ln(1-2\tilde{m}) - 4032\tilde{m}^5 \ln(1-2\tilde{m}) - \\ & 360\tilde{m}^3 \ln(1-2\tilde{m}) + 6\tilde{m} + 36\tilde{m}^2 \ln(1-2\tilde{m}) \\ & -30\tilde{m}^2 + 3\ln(1-2\tilde{m}) - \\ & 18\tilde{m} \ln(1-2\tilde{m}) \Big) \end{aligned} \tag{26}$$

This result can be improved in the case when the initial pulse is located outside the sphere $a = 10m/3$. One finds, eliminating the time derivatives of $\tilde{\Psi}$, that the energy can be written as

$$\begin{aligned} E_a(t) = 4\pi \int_a^{\infty} dr \Big(& \eta_r (\partial_r \tilde{\Psi})^2 + \frac{2(\tilde{\Psi})^2}{r^2} + \\ & \frac{20 m f^2}{r^5} (0.9 - \frac{3m}{r}) \Big). \end{aligned} \tag{27}$$

Thus $\int_a^{\infty} \tilde{\Psi}^2/r^2 dr \leq E_a/(8\pi)$ if $a > 10m/3$. As a consequence the factor in the inequality (21) halves and, finally, the formula (25) can be replaced by

$$\frac{\delta E_a}{E_a} \leq 2.25 \Big(\frac{2m}{a}\Big)^2 C(\tilde{m}) \tag{28}$$

A more careful estimate, in which the $\partial_r \tilde{\Psi}$-related term is taken into account, gives even a stronger result, with

$$\frac{\delta E_a}{E_a} \leq \frac{2.25}{1 + 0.125\eta_a} \Big(\frac{2m}{a}\Big)^2 C(\tilde{m}). \tag{29}$$

In the limit $\tilde{m} \to 0$ one arrives at

$$\frac{\delta E_a}{E_a} \leq 0.3 \Big(\frac{2m}{a}\Big)^2; \tag{30}$$

that significantly improves the former result proven in [14]. The coefficient $C(m)$ diverges at $\tilde{m} = 0.5$ but it depends rather weakly on $\tilde{m} = m/a$ in the range $(0, 0.25)$. For instance, for $m/a = 0.1$ and $m/a = 0.25$, one has $2.25C(\tilde{m})/(1+0.125\eta_a) \approx 0.39$ and $2.25C(\tilde{m})/1+0.125\eta_a) \approx 1.4$, respectively.

It can be of interest to consider the case of initial data of compact support (a, b). The simplest estimate can be obtained as follows. It is easy to see that one has

$$\frac{4\pi f^2(R,t)}{R^2} \leq E_a a \eta_R^2 F(\tilde{m}, b/a), \tag{31}$$

instead of (21). The insertion of (31) into Eq. (16) yields, after a calculation analogous to that performed above,

$$\frac{\delta E_a}{E_a} \leq 0.45 \Big(\frac{2m}{a}\Big)^2 F(\tilde{m}, b/a) \Big(1 - \frac{m}{a(a-2m)} (\frac{3}{7} - \frac{\tilde{m}}{4})\Big). \tag{32}$$

This is valid also inside the photon sphere. In the case when $(b-a)/a << \eta_a^3$, one can clearly see that the backscatter is negligible.

A simpler and much stronger estimate can be obtained, assuming that $2m << a$ and the support of initial data satisfies the condition $b - a << a$. In this case one has from (18)

$$|\frac{f(R, t=0)}{R}| \leq \left((b-a) \int_a^R dr (\frac{\tilde{\Psi}}{r})^2 \right)^{1/2}. \tag{33}$$

Here $\Psi(a) = 0$ and one can show, employing the same approach as before, that

$$\begin{aligned} |\Psi(R)| = |\int_a^R dr \partial_r \Psi| = |\int_b^R dr \partial_r \Psi| \leq \\ \sqrt{\frac{E_a}{2\pi}} \min\Big(\sqrt{R-a}, \sqrt{b-R}\Big). \end{aligned} \tag{34}$$

Thus

$$\frac{4\pi f^2(R)}{R} \leq \frac{E_a}{4} b^2 (1 - \frac{a}{b})^3. \tag{35}$$

The insertion of (35) into (16) yields (notice that the spatial integration now extends from a_t to b_t and that $(a_t - b_t)/a \approx (b-a)/a$)

$$\frac{\delta E_a}{E_a} \leq 0.5 \Big(\frac{m}{a}\Big)^2 \Big(\frac{b-a}{a}\Big)^4. \tag{36}$$

III. NUMERICAL RESULTS: ELECTROMAGNETIC FIELDS

This section reports numerical results on the backscatter. We begin with demonstrating that the effect can be strong and then discuss qualitatively its wavelength dependence.

We choose initial data generated by the function

$$\partial_t f = (R-a)^{2.01}\exp\bigl(-w(R-a)^2\bigr), \qquad R \geq a; \\ = 0 \qquad\qquad 2m \leq R < a. \tag{37}$$

There are two free parameters, a and w. The exponent 2.01 guarantees that the energy density (that depends, in particular, on $\partial_R^2 f$) vanishes at a.

The initial data have a noncompact domain, but they are very small outside a compact support. In particular, the projected one-dimensional initial energy density (the integrand of Eq. (6)) is practically of compact support. On the other hand, the function f is obtained from Eq. (37) by integration and it is constant asymptotically. Since f enters the evolution equation (4), it is responsible for the backscattering; its asymptotic constancy ensures that the effect is relatively strong. In what follows the mass m is assumed to be 1. The backscattered energy is obtained by a numerical approximation of the line integral (7).

We integrated Eq. (4) for $a = 2, 4$ and 20. Fixing the parameter a, calculations were performed for a number of $w's$. The results seem to imply that $\delta E_a/E_a$ has a single maximum at some w_*, with $\delta E_a/E_a$ being almost constant in some vicinity of w_*. The limitation inherent to the numerics does allow us to find only an approximate value of w_*; that value will be called as a "maximal" point and the corresponding value of $\delta E_a/E_a$ will be referred to as a "maximum". That terminology will be kept in the rest of Sec. III as well as in Sec. V.

A. The maximal backscattering

The strongest backscattering effect is found with the choice of parameters $a = 2$ and $w = 5 \times 10^6$. The backscattered energy has been obtained by the integration of (7) along $\Gamma_{2.0001}$ [17]. Under these conditions the value of the ratio $\delta E_a/E_a$ approximates 20.5%. The backscatter is relatively insensitive on the choice of w. Fig. 1a) shows the initial energy density for various values of w as well as the strength of the backscatter as measured by the ratio $\delta E_a/E_a$.

B. Resonant type initial data and relative-width dependence

Figs. 1b) and 1c) show the behaviour of the initial energy density that corresponds to $a = 4$ and $a = 20$, respectively, and to a number of values of w. A number assigned to a curve gives the ratio of the backscattered energy. It is obvious that in these numerical examples the strength of the backscatter is correlated with the width of the support Δ of initial data. The relative width Δ/a of the energy density is related to its spectral composition; that suggests that the effect depends on the wavelength of the initial radiation.

Numerical investigation confirms a theoretically derived conclusion that in the limit $\Delta/a \to 0$ there is no backscatter ([13]; see also Eq. (36)). In our examples small values of the ratio Δ/a correspond to $w >> 1$. We found that the ratio $\delta E_a/E_a$ monotonically decreases with w, if w is large enough. In order to demonstrate how dramatic the changes can be, we compare data concerning the case $a = 4$. If $w = 10^3$, then $\delta E_a/E_a = 4.5 \times 10^{-8}$; that is rougly 10^4 less than for $w = 1$, when $\delta E_a/E_a = 1.9 \times 10^{-4}$.

The values $w = 0.1$ (in the case of $a = 4m$) and $w = 0.001$ (in the case of $a = 20m$) correspond to "resonant" initial data. That "resonant" behaviour is rather weak; for instance in the case of $a = 4$ the change of w by a factor of 10 from the maximal case results in a relatively small, less than 50%, change of the efficiency factor $\delta E_a/E_a$ of the backscattering. In general, we can say that the "resonant" width of the initial energy density (which gives also the order of the "resonant" wavelength of the radiation, if $a >> 2$) is of the order of the distance of the radiating source from the black hole.

Fig. 1a) clearly shows, in contrast with the preceding cases, that the strength of backscatter is rather weakly correlated with the width of the support of initial data. The reason for that is that (for this set of configurations), the smaller is the width, the smaller is the distance from the horizon (and thus the redshift increases). There are two competing effects that work each against the other.

In those cases that have been studied in our paper, the backscattering is strongest at $a = 2$ and $w = 5000000$, when $\delta E_{2.0001}/E_{2.0001} = 20.5\%$. The resonant efficiency drops then by a factor of 500 when passing to another resonant case at $a = 4$ and $w = 0.1$: $\delta E_4/E_4 = .045\%$. This dramatic change is expected, since the backscattering is strongest within the sphere $R = 3m$. The largest value of $\delta E_{20}/E_{20}$ (and $w = 0.001$) is obtained for $w = 0.001$ and it reads 0.00085%. Thus the increase of a from 4 to 20 again results in a roughly 50-fold decrease of the resonant efficiencies, which is somewhat quicker than fall-off suggested by the analytic estimate (25).

C. On the comparison of analytic and numerical results

Let us comment on the comparison of the numerical data with the analytic estimates of the preceding section. The inequality (25, valid generally, is not sharp. In the

case of resonant initial data, for instance, it gives a nontrivial information only for $a = 4m$ and $a = 20m$ (Figs. 1b and 1c); the numerically obtained value of $\delta E_a/E_a$ is by three orders smaller than the analytic bounds. The formula (36), that is valid at large distances and for initial data with small relative widths, should be more efficient. The use of (36) is not allowed, strictly saying, in our case since the numerical examples do not satisfy the required assumptions concerning the compactness of initial data. In the limit of $\Delta/a \to 0$, however, the initial data have "almost" compact support and in this context it is interesting that (36) gives predictions that are comparable with numerical ones, in the case of initial data with narrow support. We will study elsewhere the question whether (and under which conditions) the analytic criteria are strict.

IV. PROPAGATION OF GRAVITATIONAL WAVES

We will search the solution of the Zerilli equation [15] in the form

$$\Psi = \tilde{\Psi} + \delta, \tag{38}$$

where δ is an unknown function satisfying the (quadrupole) equation

$$(-\partial_t^2 + \partial_{r^*}^2)\delta = V\delta + (V - 6\frac{\eta_R^2}{R^2})\left(\Psi_0 + \frac{\Psi_1}{R} + \frac{\Psi_2}{R^2}\right) + \frac{2m\eta_R}{R^4}\left[-3\Psi_1 + 2\frac{\Psi_2}{R}\right]. \tag{39}$$

Here

$$V(R) = 6\eta_R^2\frac{1}{R^2} + \eta_R\frac{63m^2(1+\frac{m}{R})}{2R^4(1+\frac{3m}{2R})^2} \tag{40}$$

and $\Psi_i(r^* - t)$, $i = 0, 1, 2$, are functions that satisfy the relations

$$\begin{aligned} \partial_t\Psi_1 &= 3\Psi_0 \\ \partial_t\Psi_2 &= \Psi_1 - m\partial_t\Psi_1. \end{aligned} \tag{41}$$

The combination

$$\tilde{\Psi} \equiv \Psi_0(r^* - t) + \frac{\Psi_1(r^* - t)}{R} + \frac{\Psi_2(r^* - t)}{R^2}, \tag{42}$$

which represents a purely outgoing radiation, solves the Zerilli equation in Minkowski space-time (m=0). We choose $\Psi = \tilde{\Psi}$, $\partial_t\Psi = \partial_t\tilde{\Psi}$, which implies $\delta = \partial_t\delta = 0$ at $t = 0$.

The initial energy density multiplied by R^2 reads

$$\rho = \big((\partial_t\Psi)^2 + (\partial_{r^*}\Psi)^2 + V\Psi^2\big)/\eta_R. \tag{43}$$

The initial data are assumed to be smooth and to be nonzero outside a sphere of a radius $a > 2m$. Thus ρ is smooth and it vanishes on the boundary a. The energy content inside a part of a Cauchy hypersurface Σ_t that is exterior to a ball of a radius R can be defined as

$$E(R, t) \equiv \int_R^\infty dr\rho(r, t). \tag{44}$$

We omit a normalization constant in the definition of the energy $E(R, t)$, since we will be interested only in the relative efficiency of the backscatter and the normalization factor cancels out. The total initial energy corresponding to the hitherto defined initial data will be written as E_a.

The energy loss, that is the amount of energy that diffused inward $\tilde{\Gamma}_a$ is equal to a line integral along $\tilde{\Gamma}_a$,

$$\delta E_a \equiv E(a, 0) - E_\infty = \int_a^\infty dr\left[\eta_r\Big(\frac{1}{\eta_R}(\partial_t + \partial_{r^*})\delta(R, t)\Big)^2 + \frac{V\delta^2}{\eta_r}\right]. \tag{45}$$

It is necessary to point out that in the case of the initial point $R_0 > a$ the result would be more complicated; the differentiation of the energy along $\tilde{\Gamma}_{R_0}$ would depend also on Ψ_0, Ψ_1 and Ψ_2. If, however, the outgoing null geodesics is $\tilde{\Gamma}_a$, then it starts from a where Ψ_0, Ψ_1 and Ψ_2 do vanish. Since these functions depend on the difference $r^* - t$, their values along outgoing geodesics are constant, and that allows one to conclude that they vanish at $\tilde{\Gamma}_a$.

The fraction of the energy that could diffuse through the null cone $\tilde{\Gamma}_a$ satisfies [16]

Theorem. The efficiency of the backscattering, $\delta E_a/E_a$ satisfies the inequality

$$\frac{\delta E_a}{E_a} \le 54.5 \times \Big(\frac{2m}{a}\Big)^2 + O(m^3/a^3). \tag{46}$$

In the case of compact initial pulses one has [16], assuming $(b - a)/a << 1$ and $m/a << 1$,

$$\frac{\delta E_a}{E_a} \le \Big(\frac{2m}{a}\Big)^2\Big(\frac{b-a}{a}\Big)^4. \tag{47}$$

V. NUMERICAL RESULTS: GRAVITATIONAL FIELDS

Below we shall describe numerical results on the backscattering of even-parity gravitational waves. As in the case of electromagnetic fields, initial data are found that give rise to the strongest effect and then the wavelength dependence is discussed. Finally, the efficiency coefficient $\delta E_a/E_a$ corresponding to resonant initial data is shown to decrease with the increase of a distance.

We choose initial data generated by the function

$$\Psi_1 = (R-a)^{2.01}\exp\bigl(-w(R-a)^2\bigr), \qquad R \geq a;$$
$$= 0 \qquad\qquad 2m \leq R < a. \qquad (48)$$

The exponent is taken to be 2.01, in order to guarantee that the initial energy density (that involves second derivatives of Ψ_1) vanishes at $R = a$. There are two parameters, a and w. The initial data are of noncompact support but from the numerical point of view they are zero outside a compact set. The one-dimensional projected initial energy density (43) becomes negligibly small outside a compact support. The function Ψ_2 is obtained by integration (compare (48) and (41)) and it is constant asymptotically. Ψ_1 and Ψ_2 appear in the evolution equation (4). They probably generate the dominant contribution to the backscattering and the constancy of Ψ_2 at spatial infinity can ensure the best conditions for having the strongest effect. We put $m = 1$. As in Sec. III, Eq. (4) is integrated for $a = 2, 4$ and 20. The initial energy is calculated from the formula (44) and the backscattered energy is found numerically from Eq. (45). For each fixed parameter a is determined a value w at which the factor $\delta E_a/E_a$ is the largest one (but see the explanation in Sec. III).

A. The maximal backscattering

The highest ratio $\delta E_a/E_a$ is found for parameters $a = 2$ and $w = 10^4$. The backscattered energy was calculated along $\tilde{\Gamma}_{2.001}$ [17] and then it was noticed that $\delta E_{2.001}/E_{2.001} \approx 47\%$. Let us point out that this exceeds by a factor of 10 a prediction made in [18]. The backscatter does not depend strongly on w. Fig. 2a) shows the initial energy density for various choices of w. A number assigned to a particular curve shows the strength of the backscatter - the corresponding value of $\delta E_{2.001}/E_{2.001}$.

B. Resonant backscatter, relative width dependence and analytic estimates

Figs. 2b) and 2c) show the initial energy density at $a = 4$ and $a = 20$, for a selection of values of w, with numbers showing values of the fraction of the backscattered energy that are associated with particular initial data. Figs. 2b) and 2c) reveal that the strength of the backscatter is correlated with the relative width Δ/a of the support of initial data. In contrast with that, Fig. 2a) shows a rather weak dependence of $\delta E_a/E_a$ with the (initial) relative width. The explanation for that anomalous behaviour is as in the case of Fig. 1a - that there do appear contradictory effects - the diminishing of the relative width (with w being increased) goes in pair with the decrease of the distance from the horizon.

The efficiency of the backscatter quickly diminishes with the decrease of Δ/a, as theoretically predicted [16]. In our numerical examples the ratio Δ/a becomes smaller if w increases. It was found, for sufficiently large values of w, that $\delta E_a/E_a$ monotonically decreases with w. For instance, if $a = 4m$, then the change of w from 10^{-1} to 4×10^3 results in the decrease of $\delta E_a/E_a$ by a factor of 10^8: from 3.7×10^{-3} to 1.35×10^{-11}.

The values $w = 0.01$ (in the case of $a = 4m$) and $w = 0.0001$ (in the case of $a = 20m$) correspond to the maxima of the factor $\delta E_a/E_a$. Again, as in sec. III, "resonant" peaks are rather mild. In the case of $a = 4$ the change from $w = 0.1$ to $w = 0.001$ changes the efficiency from $\delta E_4/E_4 = 0.37\%$ to $\delta E_4/E_4 = 0.4\%$, whereas the maximum is 0.65% at $w = 0.01$. Notice, however, that the "resonant" width of the initial energy density (which gives also the order of the "resonant" length of the radiation, if $a >> 2m$) is now much bigger (by one order) than in the case of the electromagnetic dipole radiation.

The backscattering is strongest at $a = 2$ and $w = 10000$, when $\delta E_{2.001}/E_{2.001} = 47\%$. The efficiency decreases quickly, circa 70-fold, when the pulse is moved outside the photonic sphere to $a = 4$. Then the resonant value $\delta E_4/E_4 = .65\%$ corresponds to $w = 0.01$. At $a = 20$ and $w = 0.0001$ we found $\delta E_{20}/E_{20} = .01\%$. Thus the increase of a from 4 to 20 results in 65-fold decrease of the efficiency at resonant cases, which is more than the fall-off suggested by the analytic bound (46).

The comparison of the numerical data with the analytic estimates (46) and (47) yields conclusions similar to those made in the electromagnetic case. Again, the width independent criterion (46) is rather imprecise. In the case of $a = 20$ (Fig. 2c) the numerical value of $\delta E_a/E_a$ is circa 3 orders smaller than that predicted analytically. The prediction of the bound (47), that is valid for $a >> m$ and $b - a << a$ can be more precise.

VI. CONCLUSIONS

There took place a debate, about decade ago, on the quantitative evaluation of the backscattering of gravitational waves (see [18] and references therein). While one of the proponents was originally in favour of a very strong damping of the radiation, that was implied by the backscattering, the final conclusion was that the effect is weak and only a small fraction (of the order of a few percents) of the long-wave band of the gravitational radiation can be backscattered [18]. In the light of that the main results of this paper come as a surprise. It is quite likely that the ratio of almost 50% of the backscattered gravitational quadrupole radiation, that we find here, can be improved for more suitably chosen initial data. The same can be said about the backscatter of electromagnetic waves, where we established that this effect exceeds 20 %, for the dipole radiation.

The numerical examples of Sects. III and V confirm theoretical predictions that if the relative width of the

initial pulse tends to zero then the effect becomes negligible. This can be translated (using the so-called similarity theorem of Fourier transforms) into dependence on the asymptotic wavelength (or frequency) of the radiation [14]. The simplest argument would invoke to the Heisenberg principle, which clearly implies that the compression of the support of a function leads to the increase of the frequency scale in its Fourier transform. The analytic proofs can be deduced from formula 36) and (47) of this paper. On the other hand, in the "resonance" regime the dependence on the relative width (or, accepting the preceding arguments, on the wavelength) is rather weak, according to numerical data of Secs. III and V. That seems to be in a sharp contrast with what is known in the case of stationary processes [19].

Let us point out the difference between the manifestations of the gravitational redshift and of the backscattering. The gravitational redshift is responsible for the weakening of the intensity of a radiation, but - barring backscatter - all of the initial energy eventually reaches an asymptotic observer. In the limit of the geometric optics the gravitational redshift is the only phenomenon that can be observed. The backscattering in turn is responsible for the loss of energy, and it may be important in the case of a low-frequency radiation.

We observed in Secs III and V that the strongest effect takes place very close to the horizon. That reflects well the known fact that the bulk of the backscatter happens inside the marginally stable photon sphere $R = 3m$. As a consequence, the transport of an initial pulse from a location close to the horizon to a point behind $3m$ must be associated with a significant decrease in the efficiency. That was in fact observed in our numerical examples, both for gravitational and electromagnetic waves. This fall-off with a distance can be faster than $1/R^2$, which is typical for our analytic estimates.

The comparison of the analytic and numerical results suggests that analytic bounds ((25)and (46)) are not strict; their predictions are bigger from our numerical data by two - three orders. That gap can be made much smaller by a more suitable choice of initial data, but we do not expect that it could be nullified. The estimates (36) and (47) that are specialized to the case of small relative widths are expected to be much sharper. The analytic bounds on the efficiency of the backscatter clearly show that the effect is negligible if the initial burst is located far from the horizon, irrespective of the detailed character of initial data.

We would like to point out a new important application of the methods developed in this paper. Namely, the backscattered (or diffused, in the terminology of [13]) energy bounds from above the total energy of tails and quasinormal modes of black holes and of a class of quasinormal modes ("w-"modes) of neutron stars ([20], [21]). Therefore the present methods can be used as the first step in order to estimate the fraction of the energy of gravitational waves that can be carried by quasinormal modes in spherically symmetric spacetimes. That would give an indication of what can be expected in more realistic situations.

Acknowledgements. One of us (EM) thanks Bernd Schmidt for a discussion on quasinormal modes. This work has been supported in part by the KBN grant 2 PO3B 010 16. Z. Świerczyński thanks the Cracow Pedagogical University for the research grant.

---

[1] J. Hadamard *Lectures on Cauchy's problem in linear partial differential equations*, Yale University Press, Yale, New Haven 1923; C. Misner, K. Thorne, J. A. Wheeler, *Gravitation*, Freeman, San Francisco,1973.

[2] B. S. DeWitt and R. W. Brehme, Annals Phys. **9**, 220 (1960); W. Kundt and E. T. Newman, *J. Math. Phys.* **9**, 2193(1968); R. G. McLenaghan, *Proc. Camb. Phil. Soc.* **65**, 139(1969); W. B. Bonnor an M. A. Rotenberg, *Proc. R. Soc.* **A289**, 247 (1965); J. Bicak, *Gen. Rel. Grav.* **3**, 331(1972);

[3] R. H. Price, Phys. Rev. D **5**, 2419 (1972). J. M. Bardeen and W. H. Press, *J. Math. Phys.* **14**, 7(1973); B. Mashhoon, *Phys. Rev.* **D7**, 2807(1973);

[4] B. Mashhoon, Phys. Rev. D **10**, 1059 (1974); G. Schäfer, *Astron. Nachr.* **311**, 213(1990);

[5] L. Blanchet and G. Schaefer, Class. Quant. Grav. **10**, 2699 (1993);

[6] C. Gundlach, R. H. Price and J. Pullin, Phys. Rev. D **49**, 883 (1994) [arXiv:gr-qc/9307009];

[7] C. Gundlach, R. H. Price and J. Pullin, Phys. Rev. D **49**, 890 (1994) [arXiv:gr-qc/9307010]; L. Blanchet, *Gravitational Radiation from Relativistic Sources*, in Relativistic Gravitation and Gravitational Radiation, eds J. A. Marck and J. P. Lasota, (Cambridge University Press 1997);

[8] L. Blanchet, Class. Quant. Grav. **15**, 113 (1998) [arXiv:gr-qc/9710038];

[9] W. B. Bonnor and M. S. Piper, Class. Quant. Grav. **15**, 955 (1998) [arXiv:gr-qc/9703012];

[10] R. Mankin, T. O. Laas and R. Tammelo, Phys. Rev. D **62**, 041501 (2000).

[11] K. Roszkowski, Class. Quant. Grav. **18**, 2305 (2001) [arXiv:astro-ph/0103139].

[12] E. Malec, N. O. Murchadha and T. Chmaj, Class. Quant. Grav. **15**, 1653 (1998) [arXiv:gr-qc/9712022].

[13] E. Malec, Phys. Rev. D **62**, 084034 (2000) [arXiv:gr-qc/0005130].

[14] E. Malec, Acta Phys. Polon. B **32**, 47 (2001) [arXiv:gr-qc/0009032].

[15] Zerilli, *Phys. Rev. Lett.* **24** , 737(1970).

[16] E. Malec and G. Schafer, Phys. Rev. D **64**, 044012 (2001) [arXiv:gr-qc/0103033].

[17] The initial data are very small but they do not vanish at the initial point ($a = 2.0001$ for electromagnetic waves or $a = 2.001$ for gravitational waves) of the null cone $\tilde{\Gamma}_a$

that is being defined in Secs IIIA and VA. Therefore the integration along $\tilde{\Gamma}_a$ gives a number that is not strictly equal to δE_a but still it constitutes a valid approximation, due to the smallness of initial data.

[18] R. H. Price, J. Pullin and P. K. Kundu, Phys. Rev. Lett. **70**, 1572 (1993) [arXiv:astro-ph/9212005].

[19] J. A. H. Futtermore, F. A. Handler and F. A. Matzner in Scattering from Black Holes, Cambridge Univ. Press, Cambridge, UK 1988.

[20] H. P. Nollert and R. H. Price, J. Math. Phys. **40**, 980 (1999) [arXiv:gr-qc/9810074].

[21] K. D. Kokkotas and B. G. Schmidt, Living Rev. Rel. **2**, 2 (1999) [arXiv:gr-qc/9909058].

Karkowski et al., Fig. 1

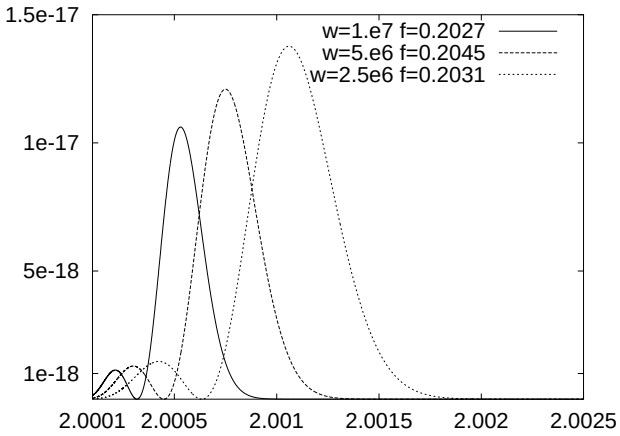

(a)

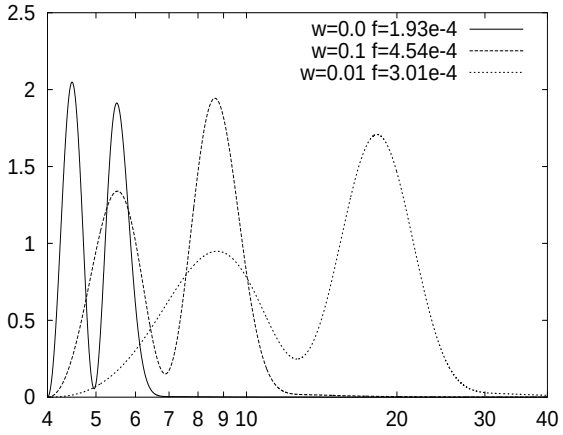

(b)

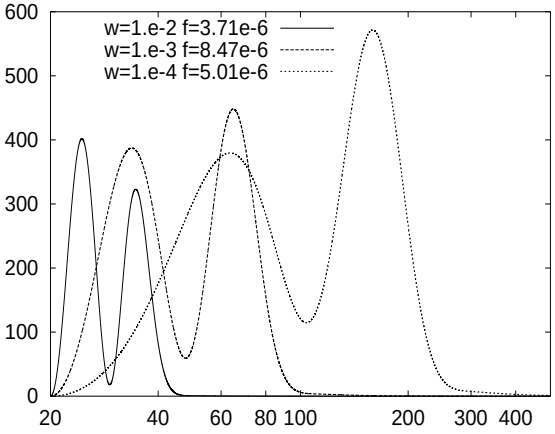

(c)

Fig.1. Initial energy densities of the electromagnetic field for various values of a ((a): a=2; (b): a=4; (c): a=20) and w. The x-axis is in the Log10 - scale. The units of the y-axis are arbitrary. Numbers "f" describe the ratio of the backscattered versus the initial energy.

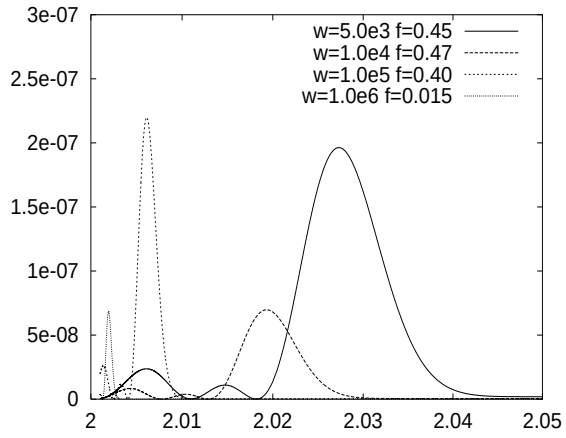
3e-07
2.5e-07
2e-07
1.5e-07
1e-07
5e-08
0
2
2.01
2.02
2.03
2.04
2.05
w=5.0e3 f=0.45
w=1.0e4 f=0.47
w=1.0e5 f=0.40
w=1.0e6 f=0.015

(a)

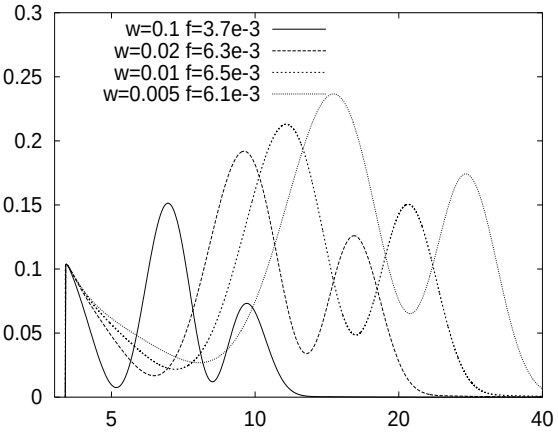
0.3
0.25
0.2
0.15
0.1
0.05
0
5
10
20
40
w=0.1 f=3.7e-3
w=0.02 f=6.3e-3
w=0.01 f=6.5e-3
w=0.005 f=6.1e-3

(b)

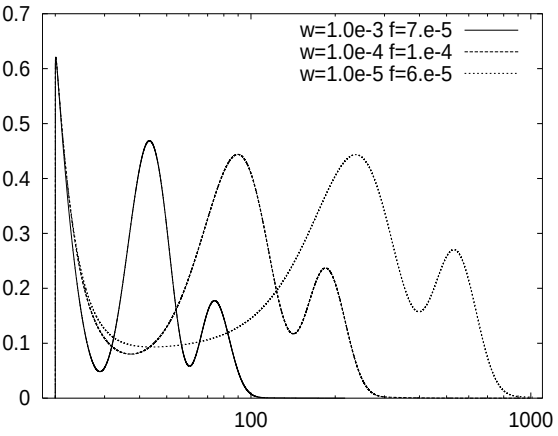
0.7
0.6
0.5
0.4
0.3
0.2
0.1
0
100
1000
w=1.0e-3 f=7.e-5
w=1.0e-4 f=1.e-4
w=1.0e-5 f=6.e-5

(c)

Fig.2. Initial energy densities of the gravitational field for various values of a ((a): a=2; (b): a=4; (c): a=20) and w. The x-axis is in the Log10 - scale. The units of the y-axis are arbitrary. Numbers "f" describe the ratio of the backscattered versus the initial energy.